Radio sources

P. Charlot
Laboratoire d'Astrophysique de Bordeaux

Outline

- Introduction
  - Continuum and spectral line emission processes
  - The radio sky: galactic and extragalactic
- History of radioastronomy
  - The first 50 years (1932-1981)
- Active Galactic Nuclei (AGN)
  - Observational properties
  - Standard unified model
- Imaging radiosources
  - Aperture synthesis
  - The case of VLBI

Radio emission processes

Electromagnetic emission can be divided into two types:

- Continuum emission
  - → emission over a very broad frequency range
  - → usually due to the acceleration of charged particles moving with a wide-range of energy

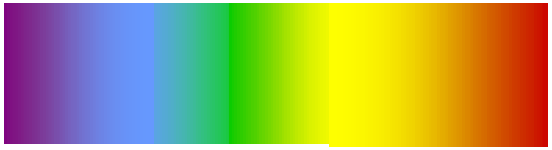

- Spectral line emission
  - → emission over a very narrow frequency range
  - → usually due to the discrete transitions in the internal energy states of atoms or molecules

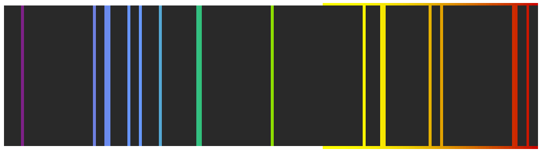

Continuum emission

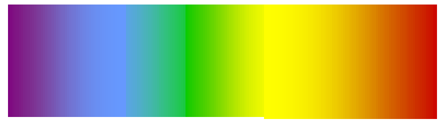

- Thermal emission
  - Black body radiation for objects with temperature T ~3-30 K
  - Bremsstrahlung (free-free) emission: deflection of a charged particle (electron) in the electric field of another charged particle (ion)

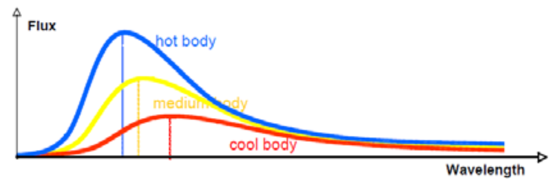

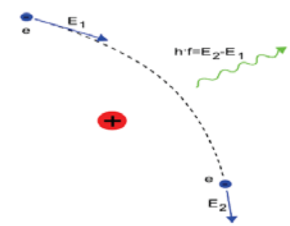

- Non-thermal emission
  - Synchrotron radiation: relativistic electrons spiraling around weak magnetic field lines

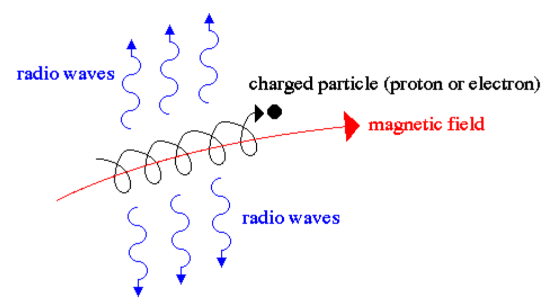

Spectral line emission

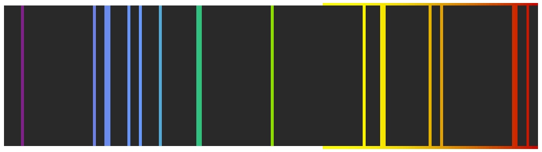

- Neutral hydrogen (21 cm)
  - spin-flip transition between high-energy state and low-energy state of the H atom (aligned vs opposed spins for p+ and e-)

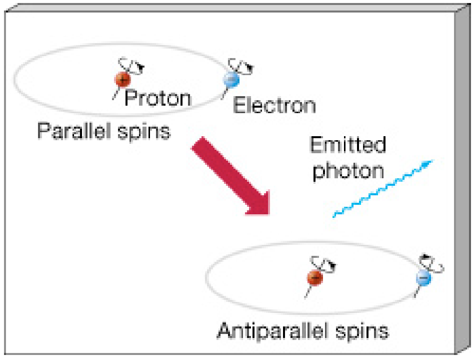

- Molecular lines (CO, CS, CN,…)
  - produced by changes in the vibrational or rotational states of their electrons (due to collisions or interactions)

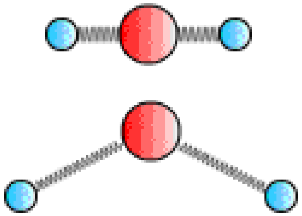

- Maser emission
  - Amplification of incident radiation passing through clouds of gas

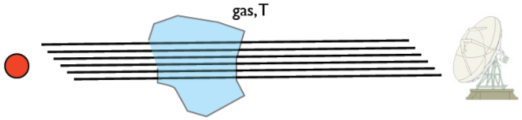

The radio sky: galactic objects

Ionized gas in the Orion nebula

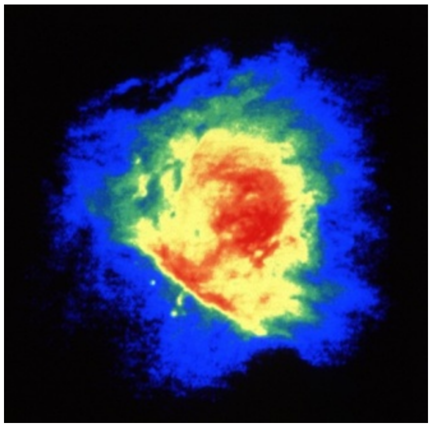

Betelgeuse

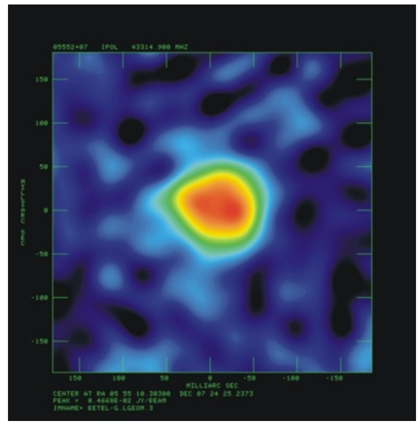

Masers around the star TX Cam

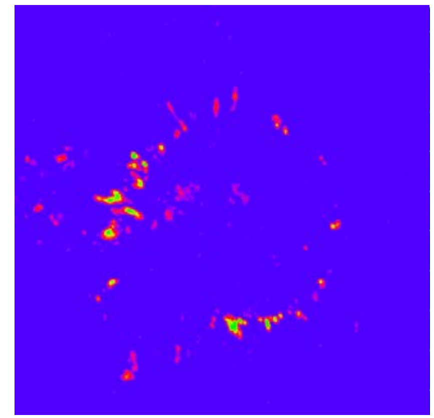

SS 433 (X-ray binary)

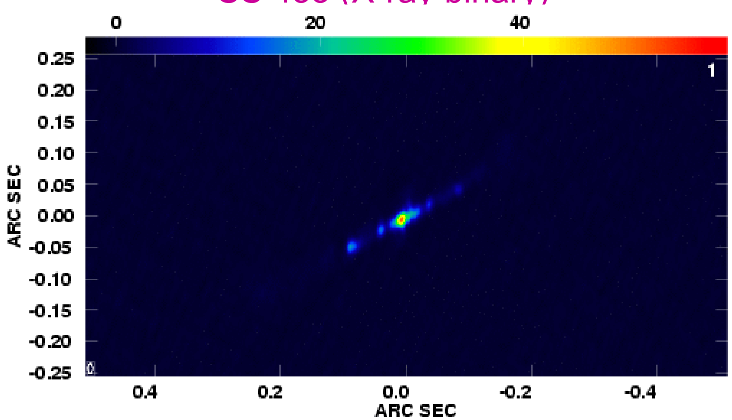

Pulsars

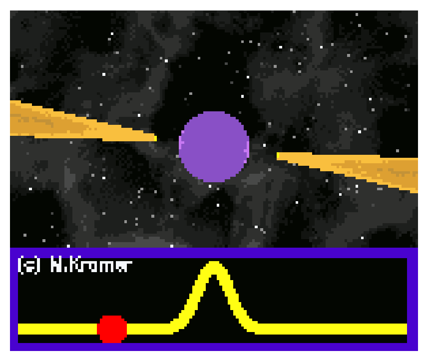

Supernova remnant

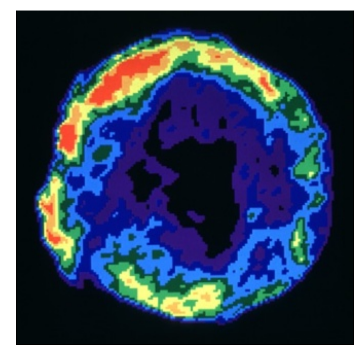

Credits: M. Kramer (pulsar animation) – all other images courtesy of NRAO/AUI

The radio sky: galaxies & AGN

Atomic hydrogen emission

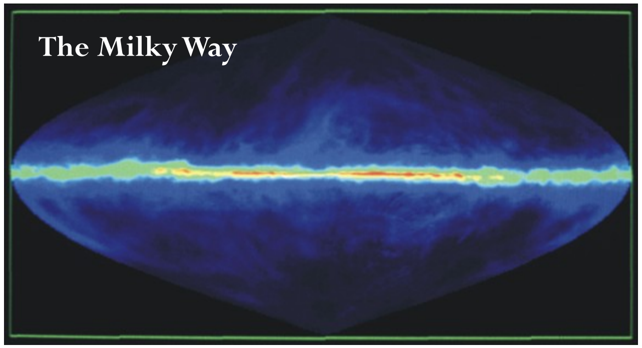

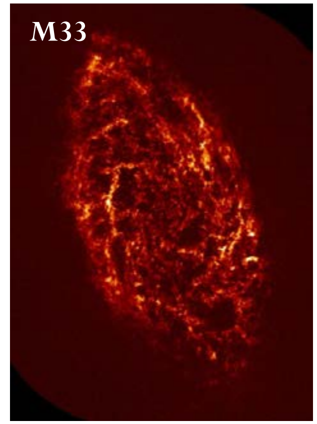

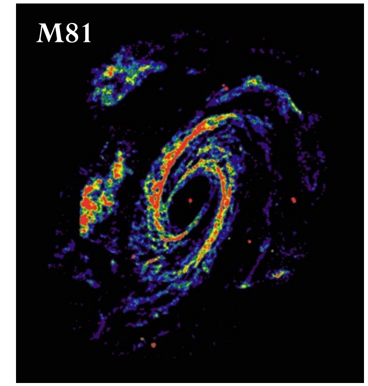

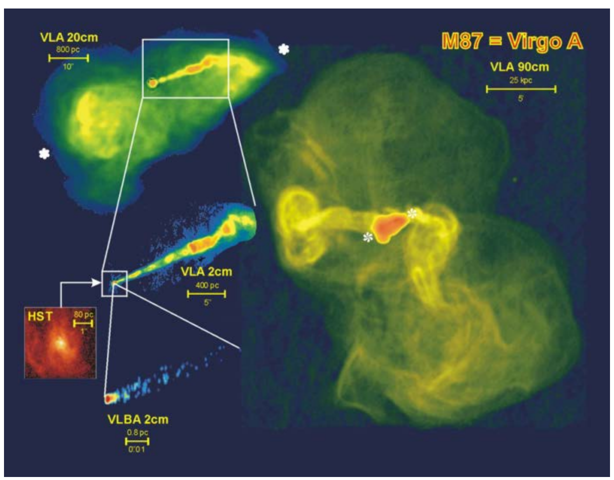

Continuum emission

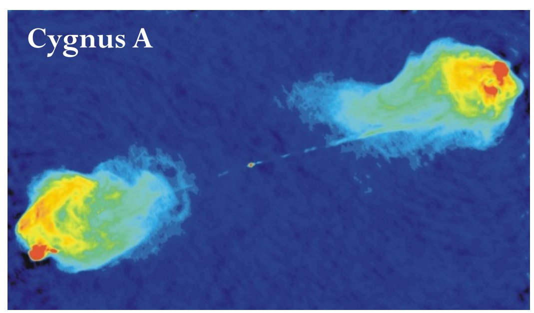

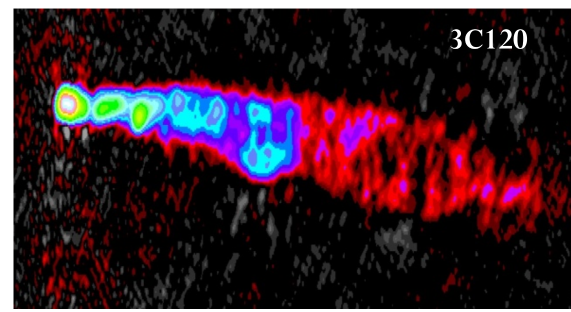

Images courtesy of NRAO/AUI

History of radioastronomy

When it all started…

- 1932: Karl Jansky discovers cosmic radio waves while investigating sources of radio noise adversely affecting transatlantic communications

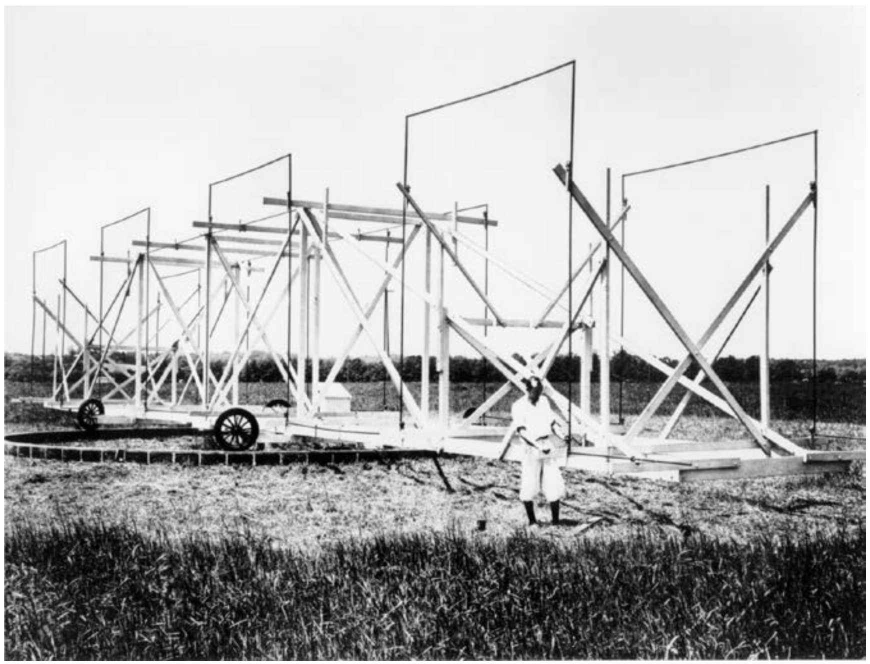

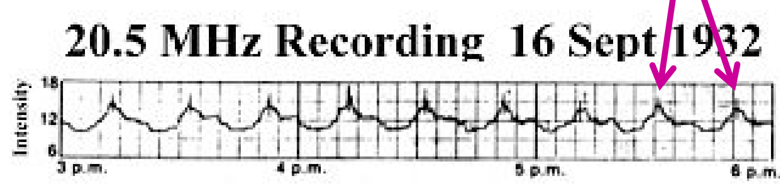

Images courtesy of NRAO/AUI

The first radio astronomer…

1944: Grote Reber builds the first parabolic radio telescope and makes the first map of the radio sky (160 MHz & 480 MHz)

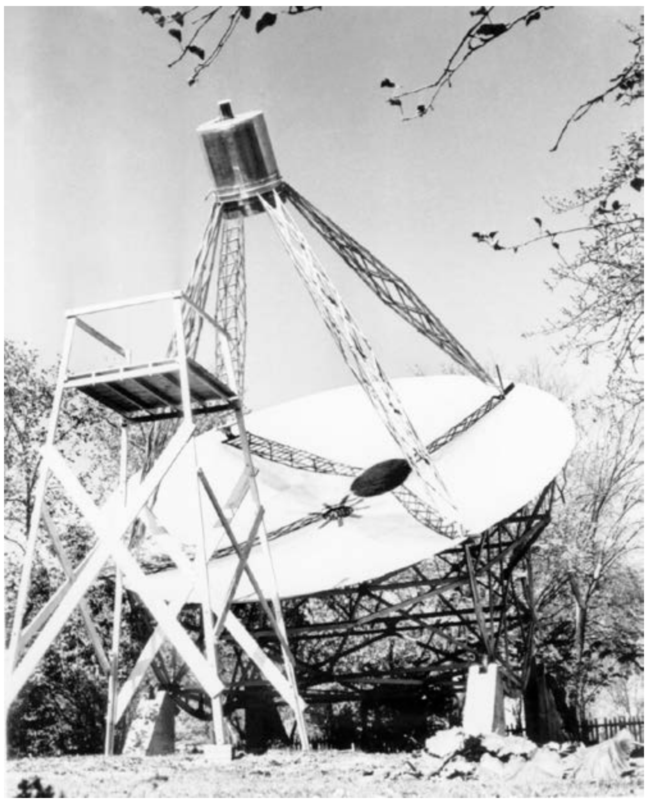

Images courtesy of NRAO/AUI

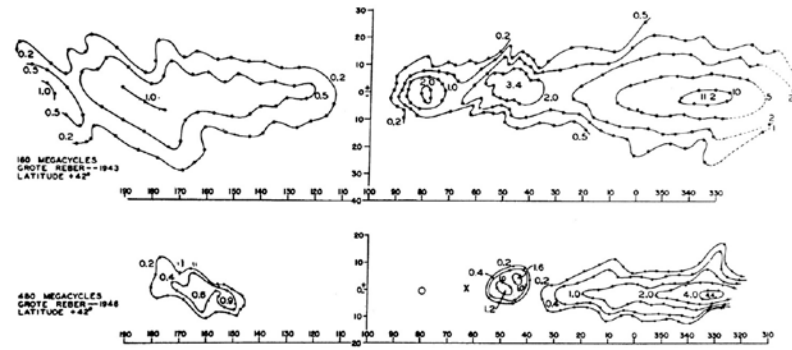

- Later on detects radio emission from Cas-A, Cyg-A, Cyg-X,…

- Multi-frequency observa-tions reveal non-thermal emission

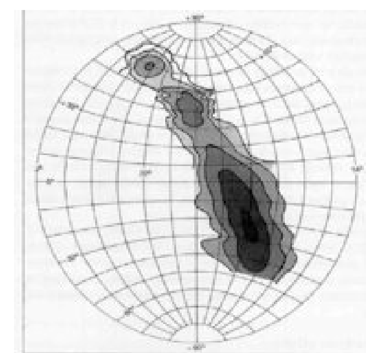

Further steps

- 1949: identification of two strong radio sources (Cen-A, Virgo A) with nearby galaxies (Bolton et al.)

- 1954: identification of the radio source Cyg-A with a distant galaxy (Baade & Minkowski)

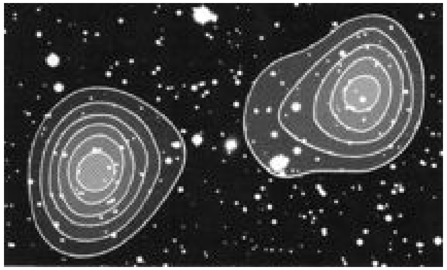

→ reveals the extragalactic nature of some of the radio sources

Two major discoveries

- 1963: discovery of quasars (quasi-stellar radio source)
  - Identification of 3C273 with a faint 13th magnitude star-like source
  - … but with emission lines shifted to longer wavelengths by 16%

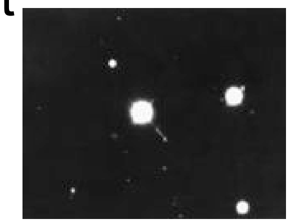

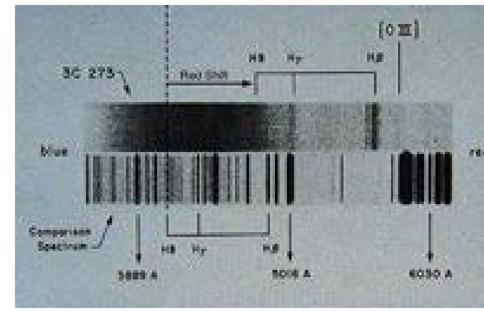

Schmidt (1963)

  → most distant known object in the Universe at the time but also intrinsically the most luminous one.

  → first member of a new class of objects now referred to as « Active Galactic Nuclei » (AGN)

- 1967: discovery of pulsars
  - Periodic source of radio emission with T=2s
  - associated with dense fast rotating neutron star

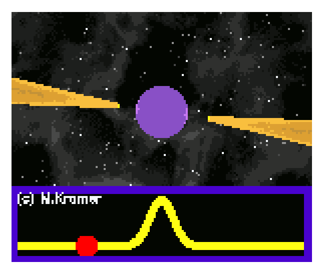

Credit: M. Kramer

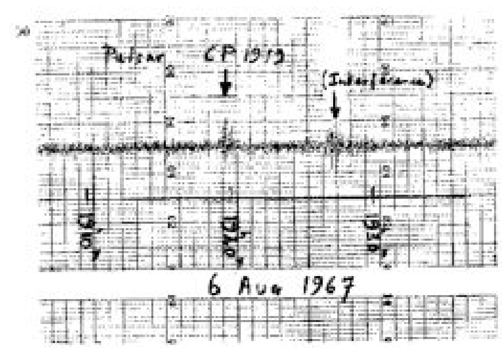

Bell & Hewish (1968)

A VLBI-specific discovery

- Apparent faster-than-light motions in AGN (known as superluminal motions)
  - 1971: through visibility curves (Whitney et al.)
  - 1981: through VLBI imaging (Pearson et al.)

- Interpreted as a geometrical effect in a relativistically-expanding source

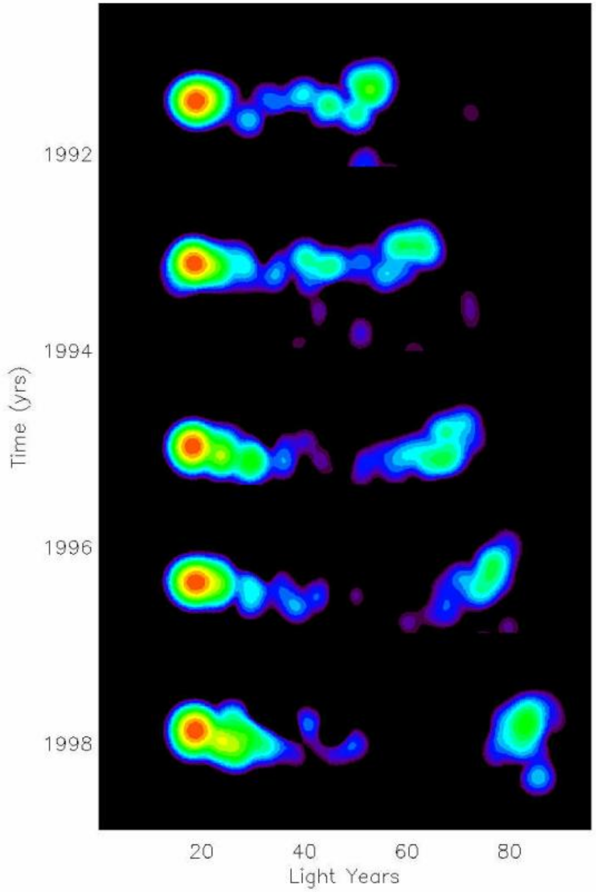

Images courtesy of NRAO/AUI

Active Galactic Nuclei (AGN)

AGN distances

- AGN are located at cosmological distances
- Distance is measured by redshift: $\mathbf{z = \lambda - \lambda_0 / \lambda_0}$

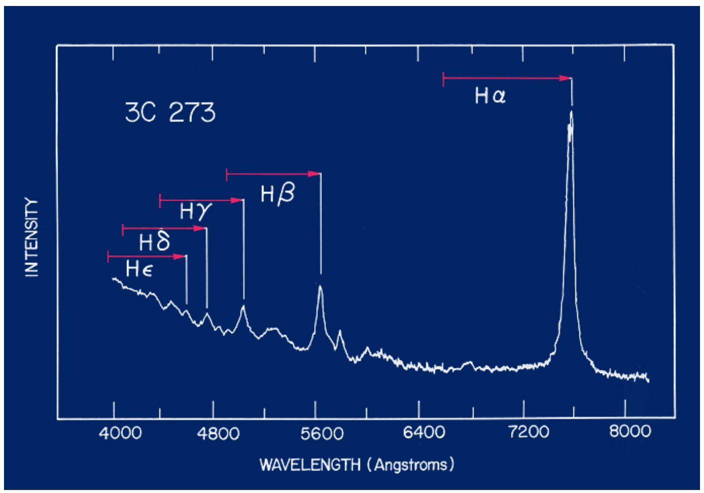

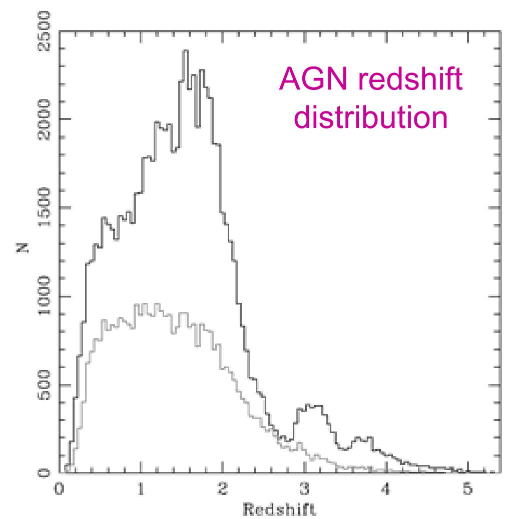

Schneider et al. (2007)

- highest-redshift quasar known at present is at z=7.085 while the highest-redshift radio source is at z=6.21
- AGN have no detected proper motions

AGN spectra

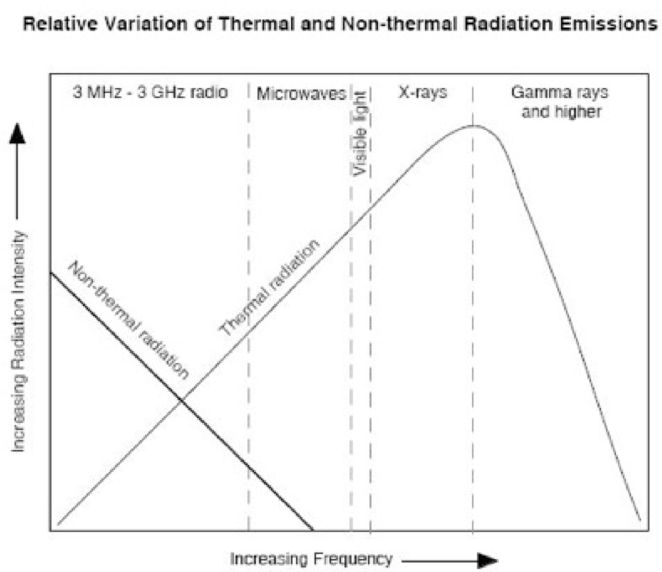

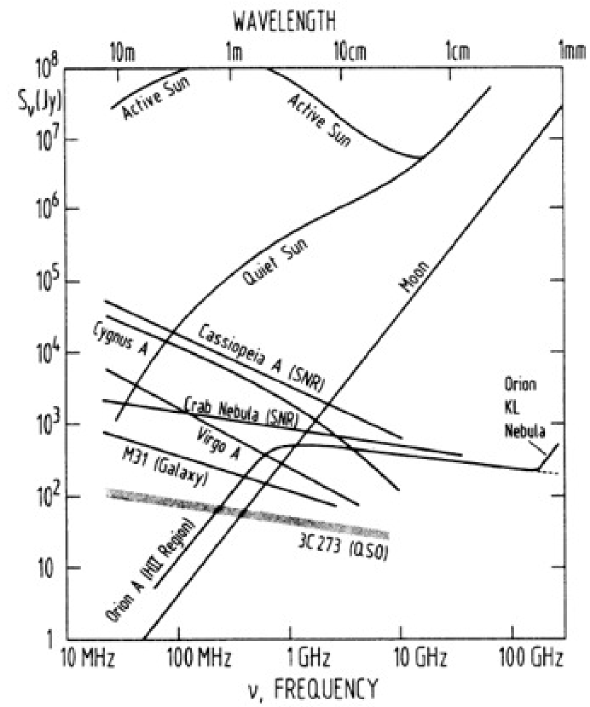

- Non-thermal emission
- About 15-20% of AGNs are « radio-loud » while the rest are « radio-quiet »

AGN variability

AGN may vary at any wavelength (from radio to gamma-rays) on timescales of minutes to years

Years

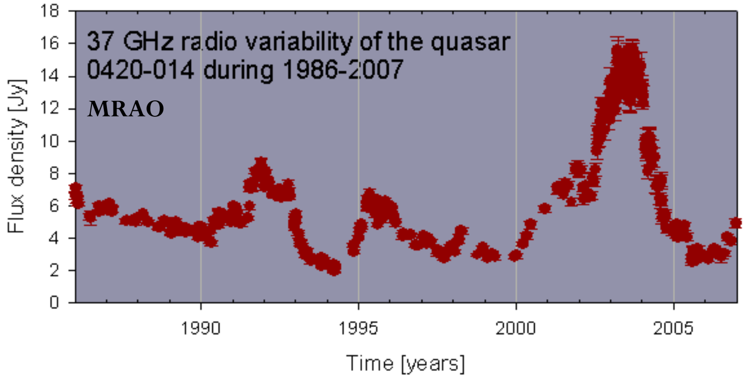

Months

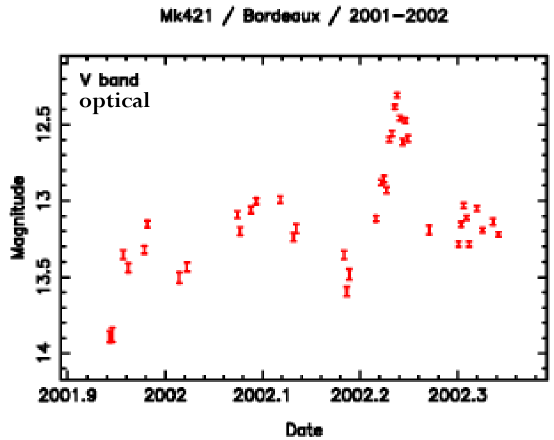

Years

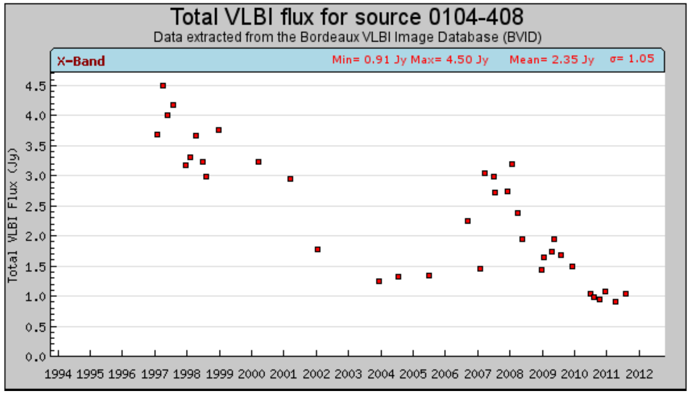

Hours

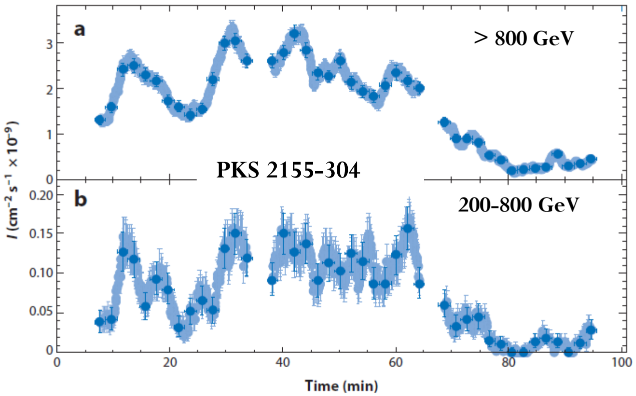

Aharonian et al. (2008)

AGN size

Intrinsic fast variations imply very small physical size for the variable region

- An object that shows variability on a timescale Δt cannot be larger than c Δt.

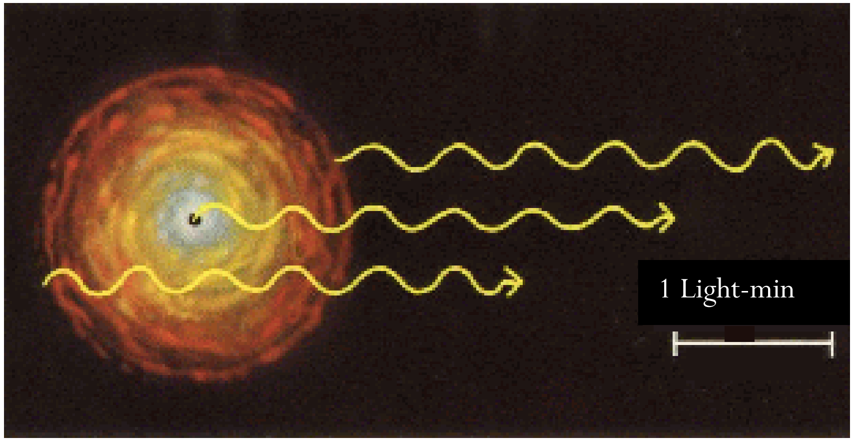

Credit: Gene Smith

- Variability on a scale of a few minutes means that the AGN size cannot be larger than a few light-minutes.

VLBI morphology

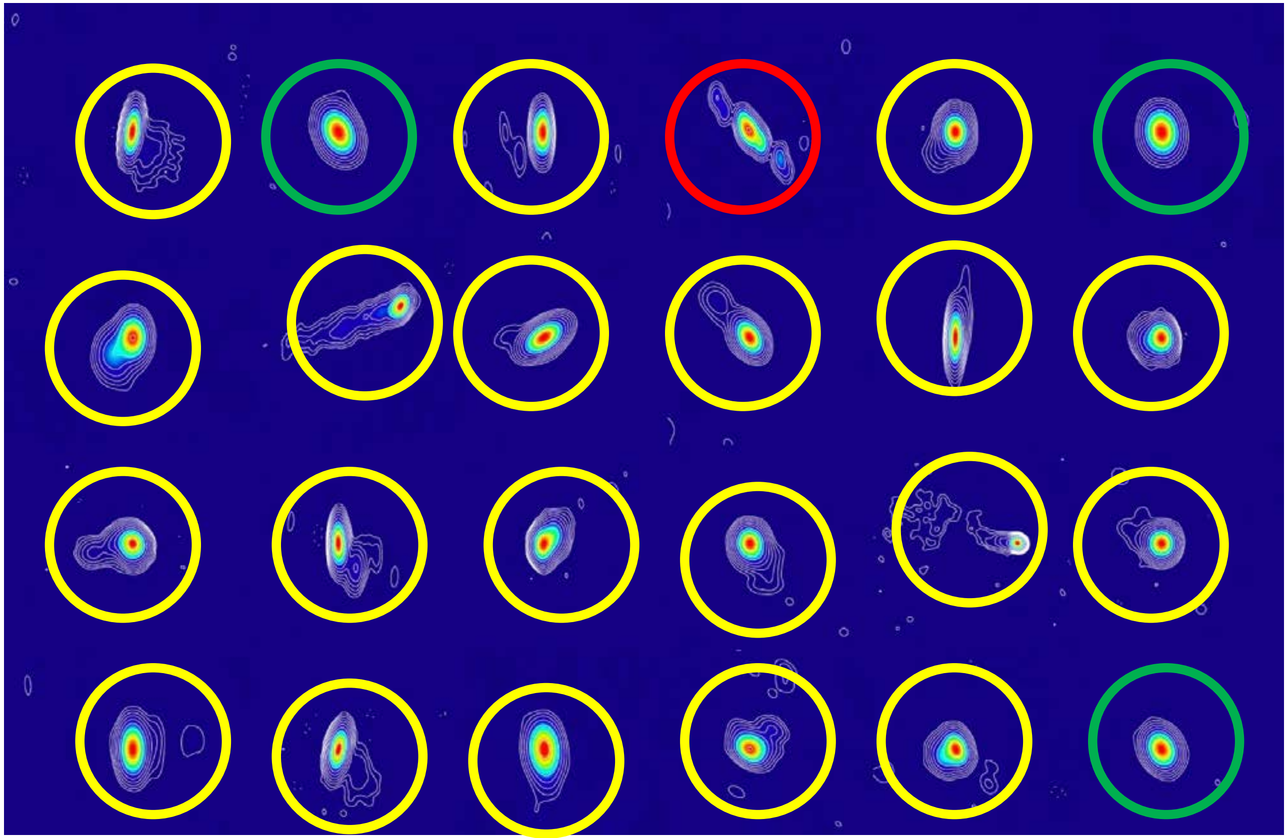

A sample of X band (8 GHz) VLBI maps with milliarcsecond resolution picked up randomly from the *Bordeaux VLBI Image Database (BVID)*

BVID
Bordeaux VLBI Image database

- Point-like
- One sided
- Two-sided

Time evolution

3C120

2000

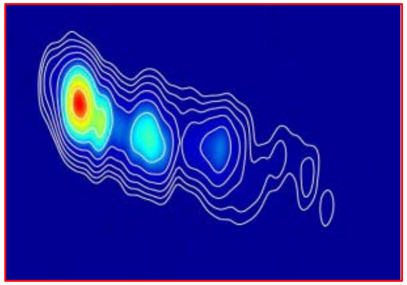

2001

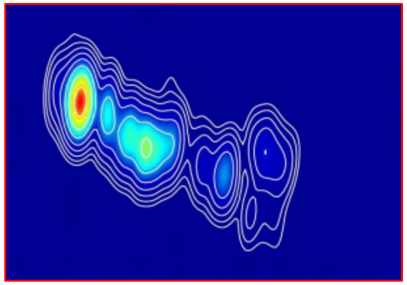

2003

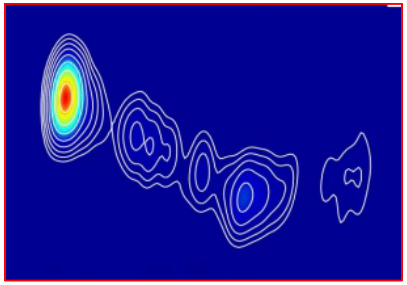

Credit:
Bordeaux VLBI
Image Database

2234+282

2000

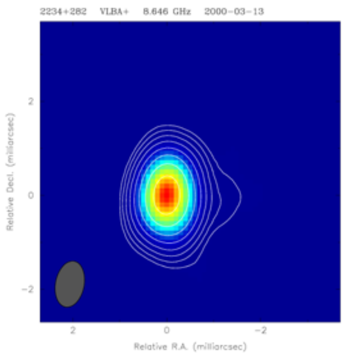

2001

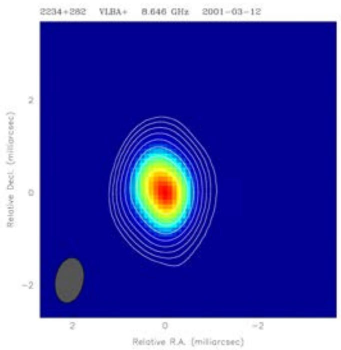

2003

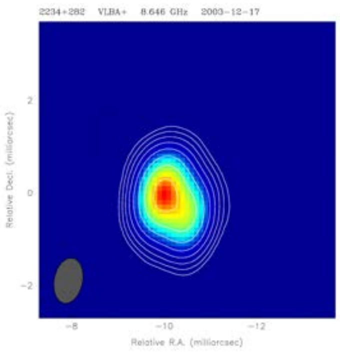

2007

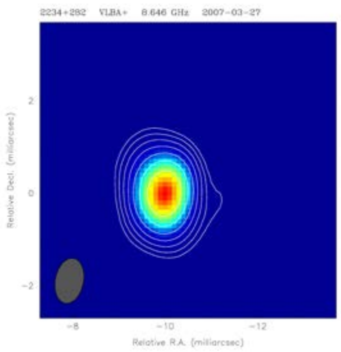

VLBI movies

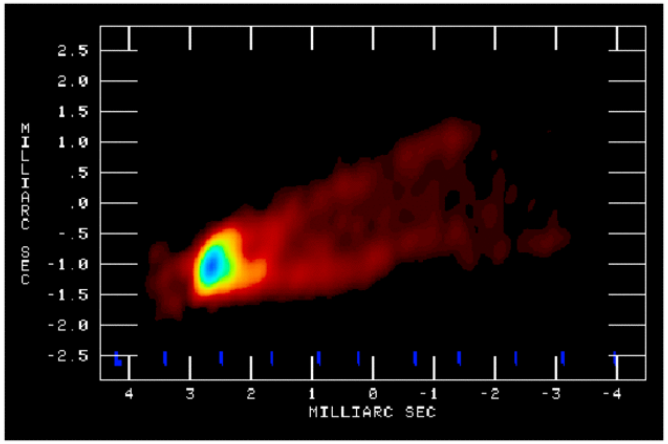

Credit: Craig Walker

Credit: MOJAVE database

Credit: MOJAVE database

Credit: MOJAVE database

AGN standard unified model

Major components

- Black hole
- Accretion disk
- Torus
- Pair of relativistic jets

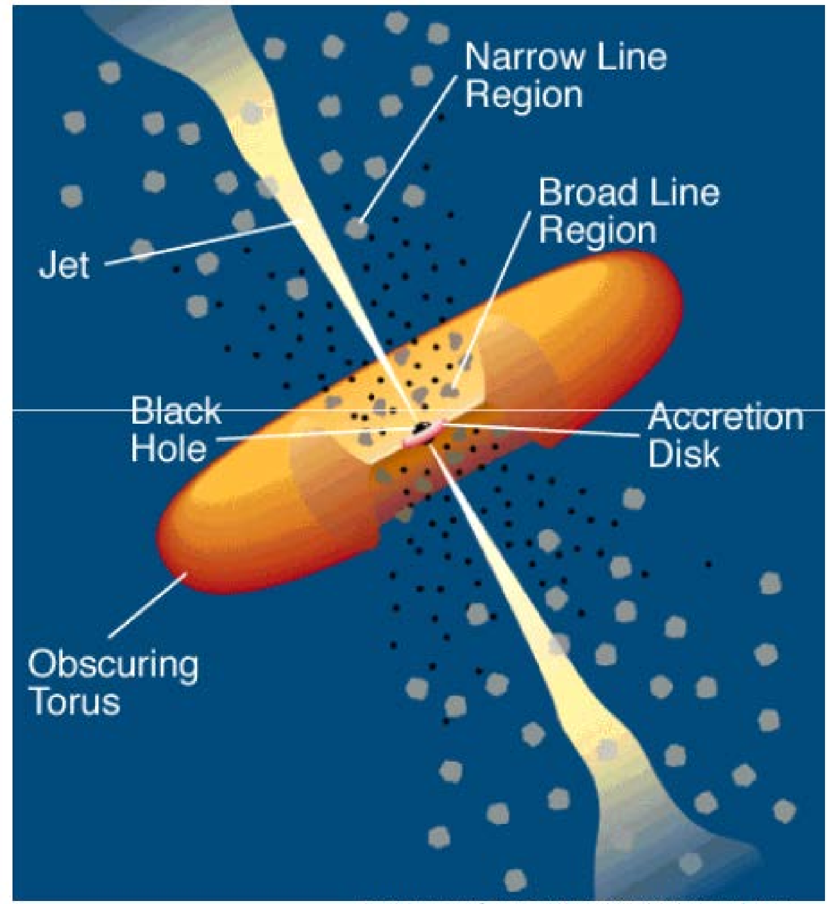

http://heasarc.gsfc.nasa.gov/docs/objects/agn/agn_model.html

Credit: C.M. Urry & P. Padovani

Impact of viewing angle

Object with jet close to the plane of the sky

- weak core
- two-sided jet

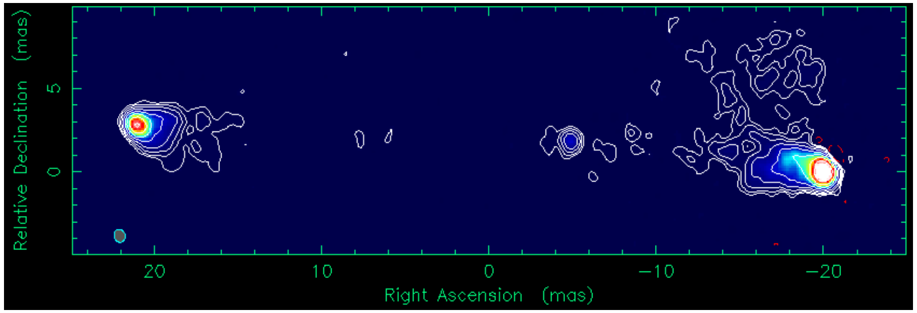

Polatidis et al. (1999)

Object with jet pointing towards the observer

- strong core
- one-sided jet

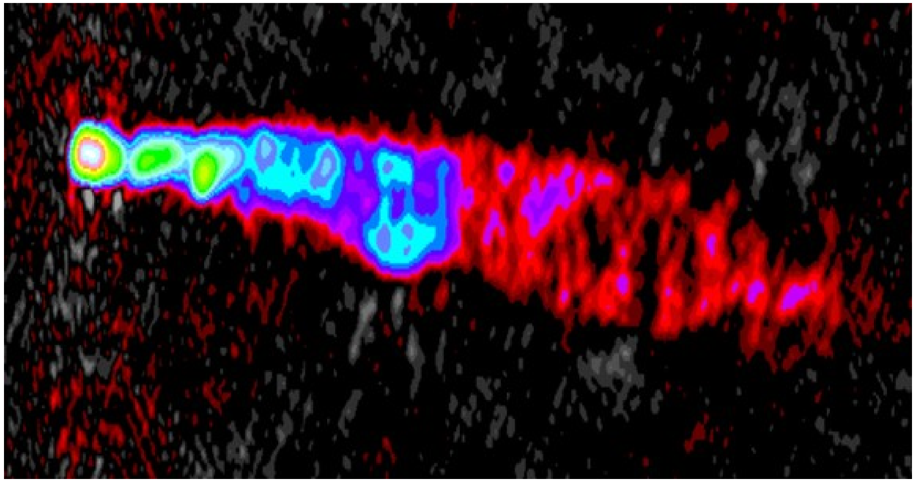

Image courtesy of NRAO/AUI and R. C. Walker

The AGN zoo

- Dichotomy radio-loud/ radio quiet
- Classification according to viewing angle
  - Radio loud: BL Lac, quasars, radio galaxies
  - Radio-quiet: QSO, Seyfert 1, Seyfert 2

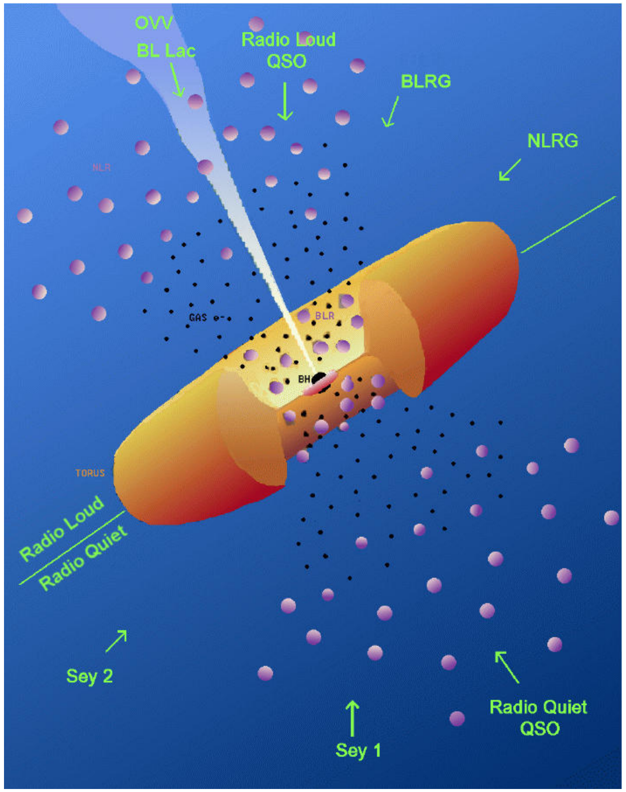

Credit: C.M. Urry & P. Padovani

Emission mechanisms in AGN

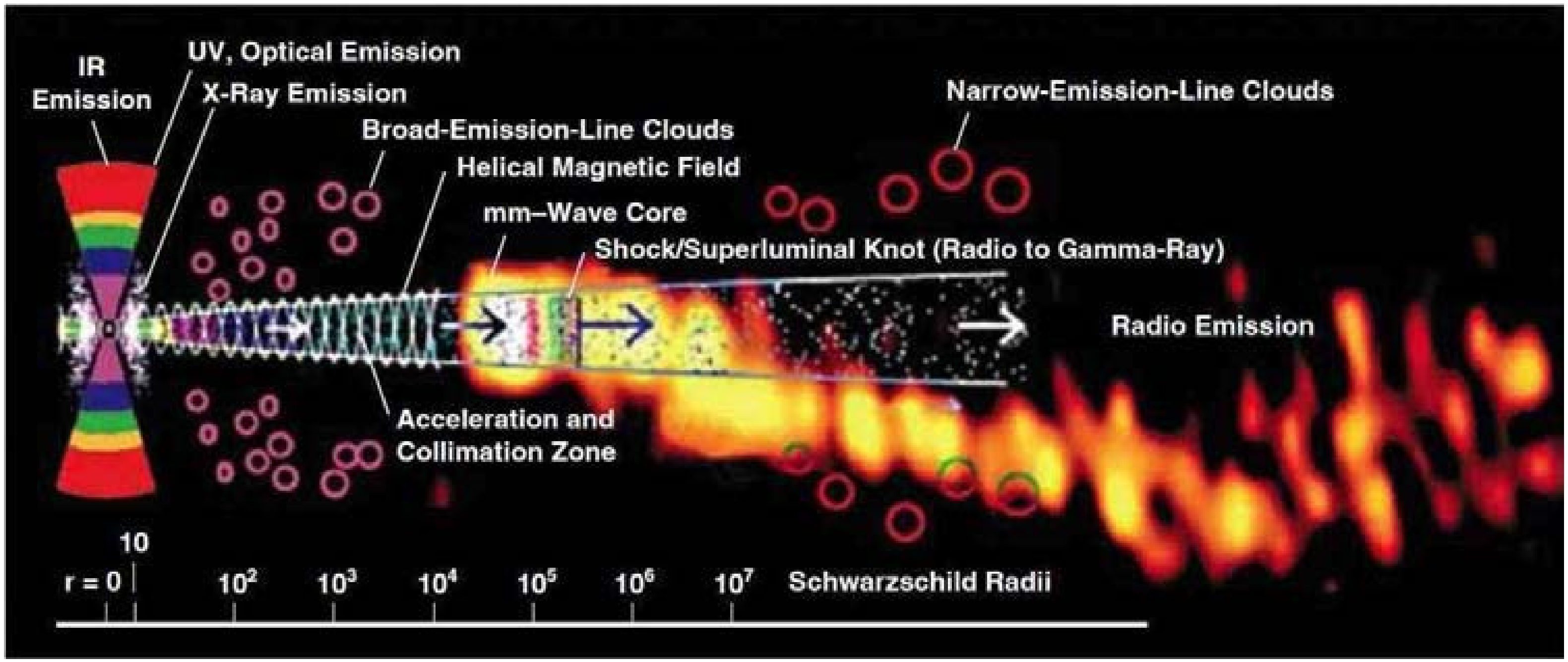

Credit: Alan Marscher

Jet properties

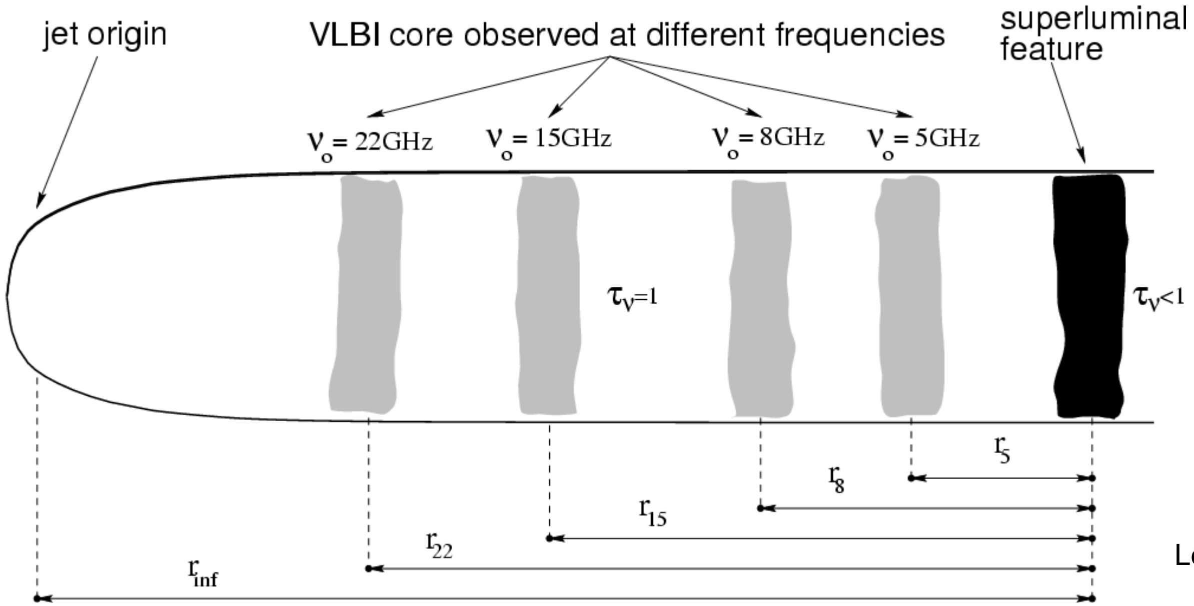

Lobanov (1996)

- Core emission not superimposed at different frequencies.
- Jet emission less prominent as frequency increases

Source structure vs frequency

2 GHz

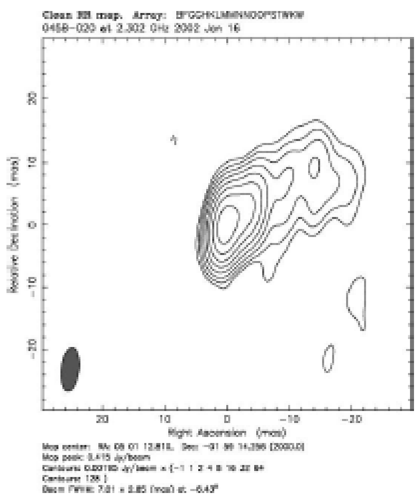

8 GHz

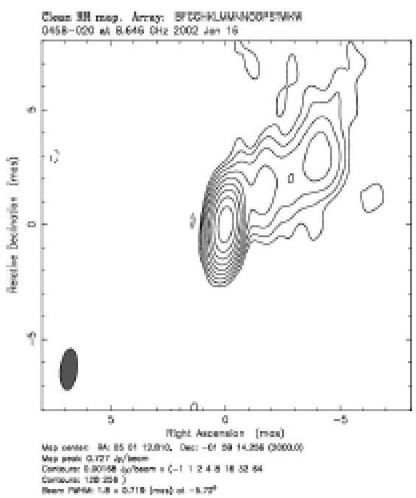

24 GHz

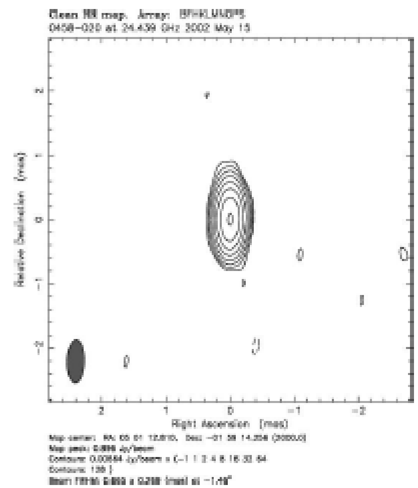

43 GHz

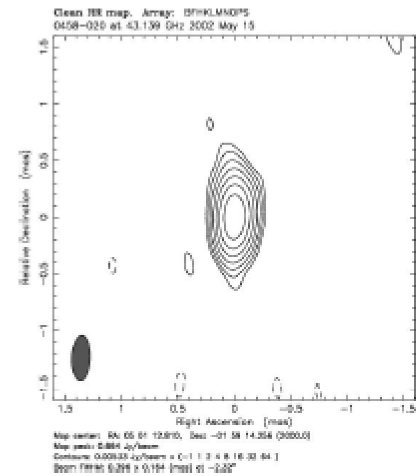

Credit: Radio Reference Frame Image Database

➔Source structure gets more compact at higher frequencies

Astrometric implications

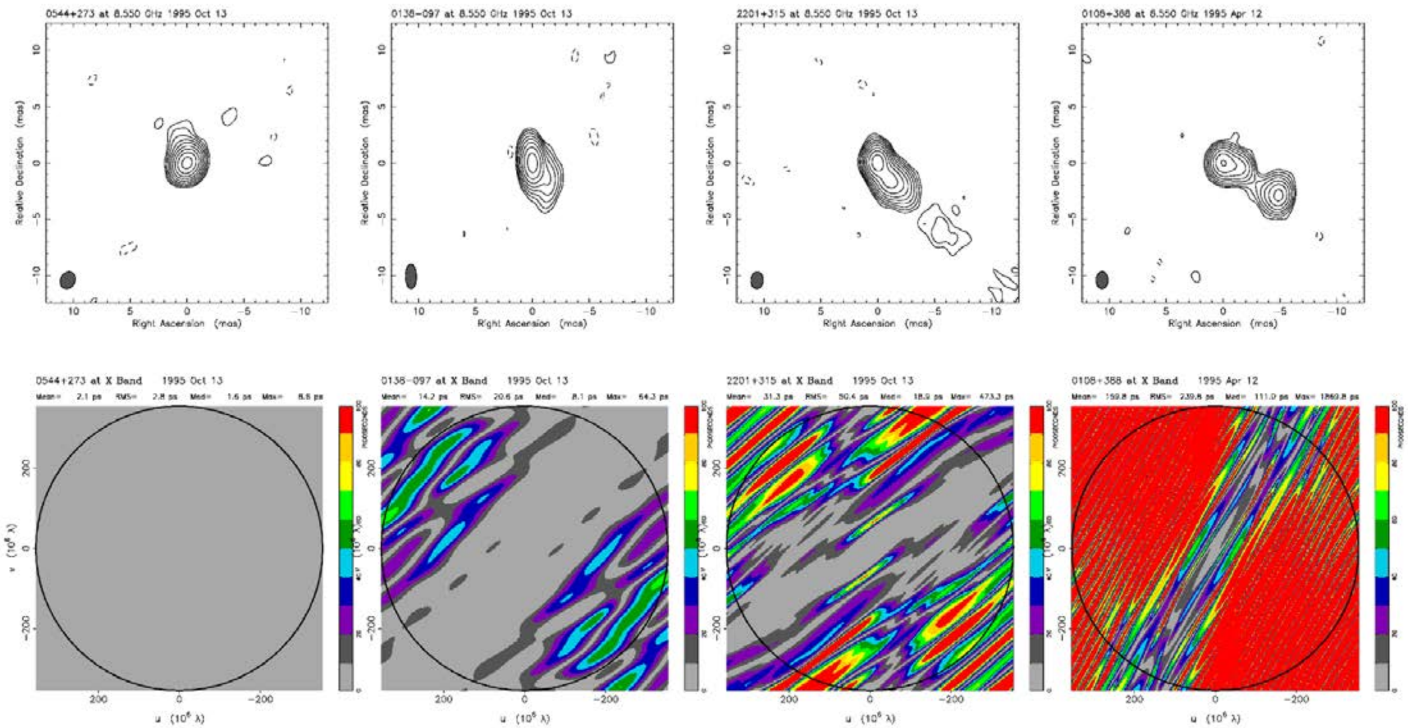

Source structure effect in VLBI delay

SI = 1
Excellent

SI = 4
Very bad

The structure index (SI) – defined as the median « source structure effect » over the u-v plane – indicates the astrometric suitability of the sources.

Imaging radiosources

Aperture synthesis: principle

Complex visibility

$$V(u,v) = A \exp(i\,\Phi) = \iint_S I(x,y) \exp(-2\pi i(ux+vy))\, dx dy$$

- u,v (measured in wavelengths) are spatial frequencies in E-W and N-S directions, i.e. the baseline length
- x,y (measured in radians) are angles in tangent plane relative to a reference position in the E-W and N-S directions

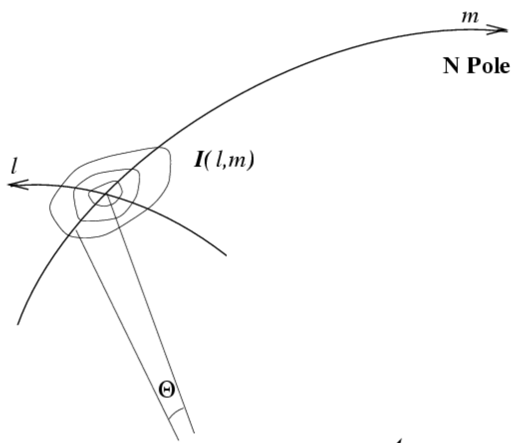

Sky brightness

$$I(x,y) = \iint_{\text{plan }(u,v)} V(u,v) \exp(2\pi i(ux+vy))\, du dv$$

- The complex visibility is the 2D Fourier transform of the brightness on the sky

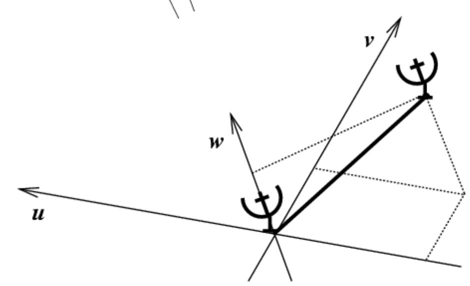

Credit: David Wilner

Amplitude and phase

- Amplitude tells « how much » of a certain frequency component
- Phase tells where this component is located

I (x,y) A {V(u,v)} Φ {V(u,v)}

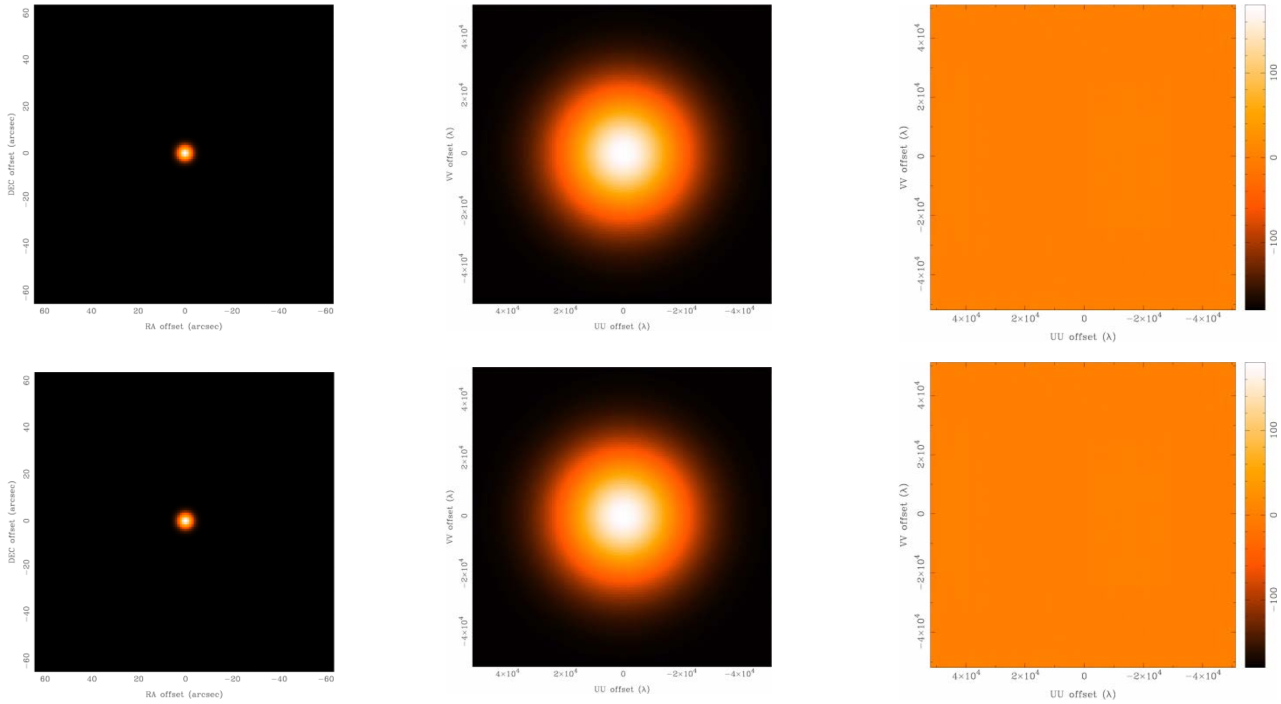

Credit: David Wilner

Amplitude and phase

- Amplitude tells « how much » of a certain frequency component
- Phase tells where this component is located

I (x,y) A {V(u,v)} Φ {V(u,v)}

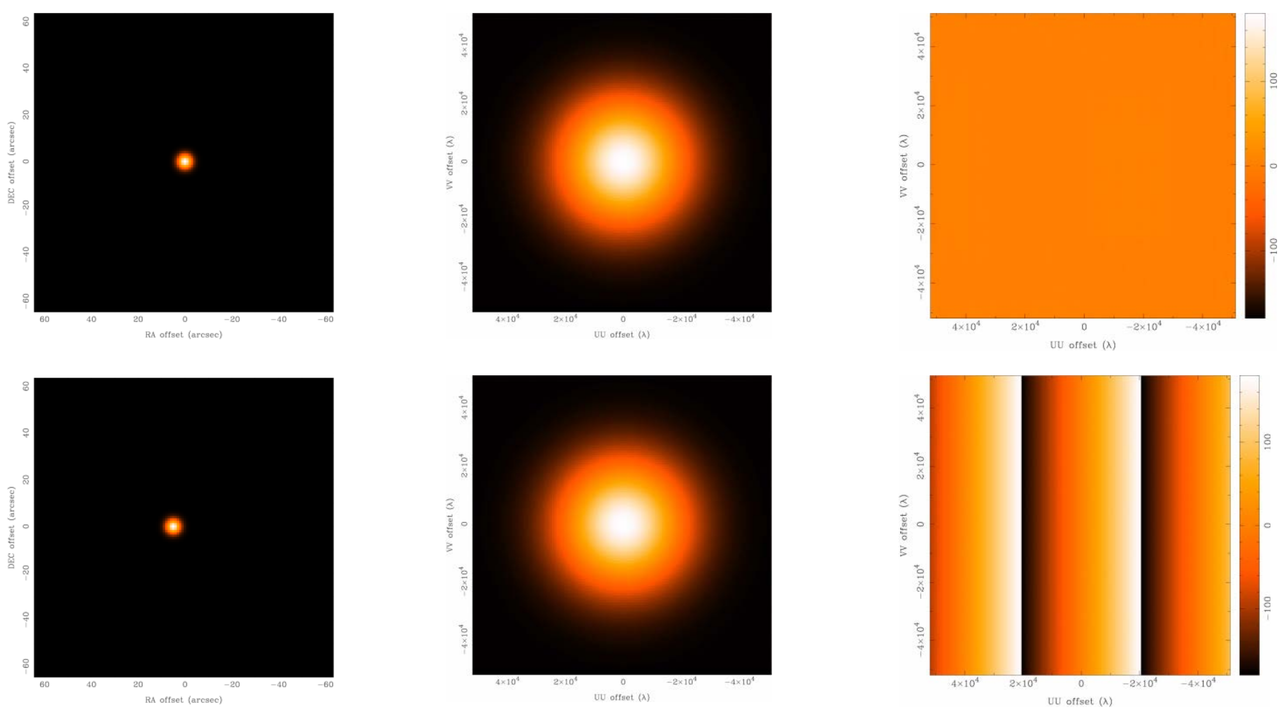

Credit: David Wilner

Amplitude and phase

- Amplitude tells « how much » of a certain frequency component
- Phase tells where this component is located

I (x,y) A {V(u,v)} Φ {V(u,v)}

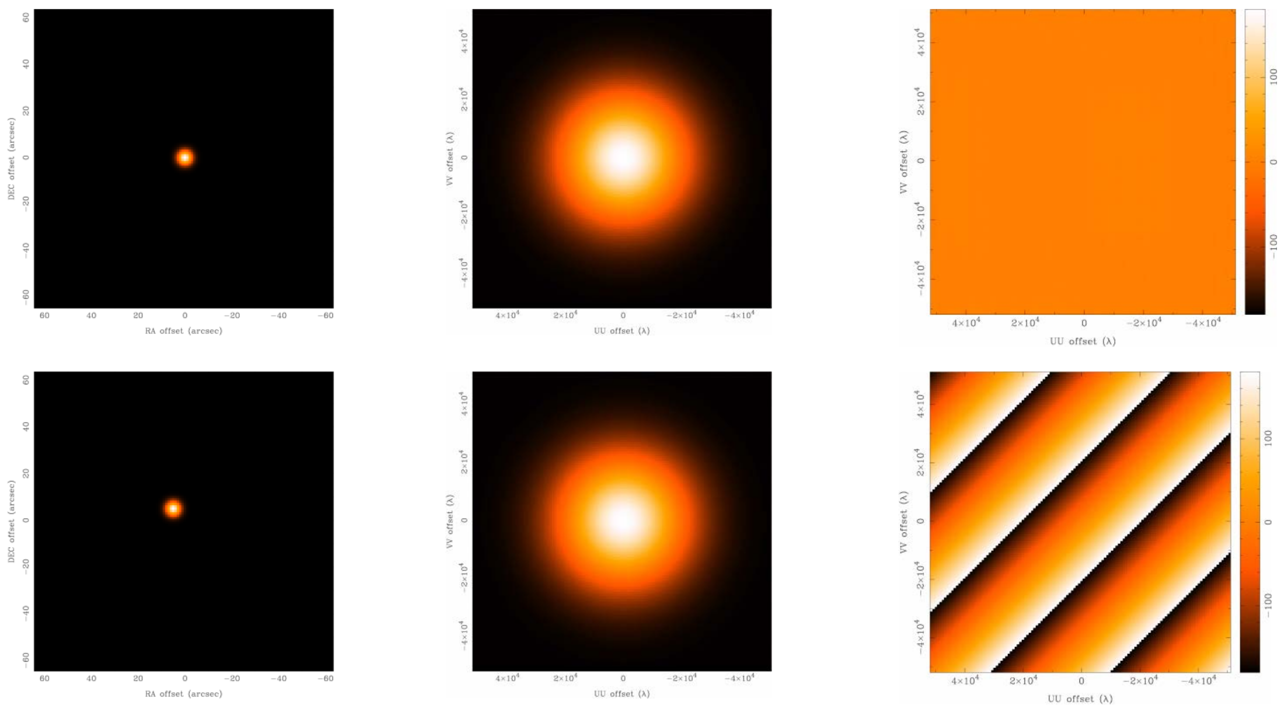

Credit: David Wilner

Aperture synthesis: ideal case

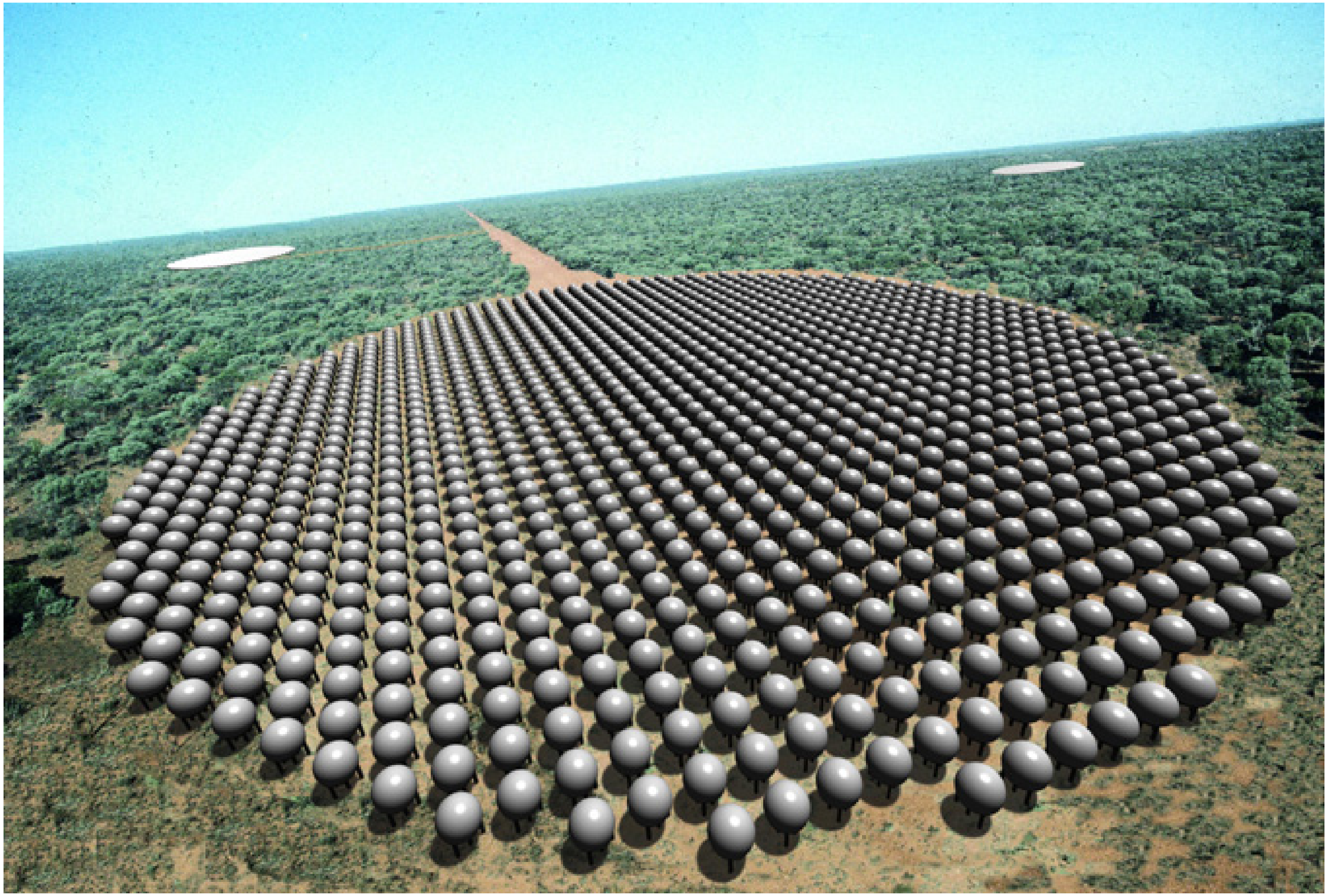

Aperture synthesis: real life

In practice, the (u,v) plane is incompletely covered and only a limited number of spatial frequencies is sampled

$$I(x,y) = \sum_{j=1,N} V(u_j, v_j) \exp(2\pi i(u_j x + v_j y))$$

➔ Image distortion

➔ Needs deconvolution

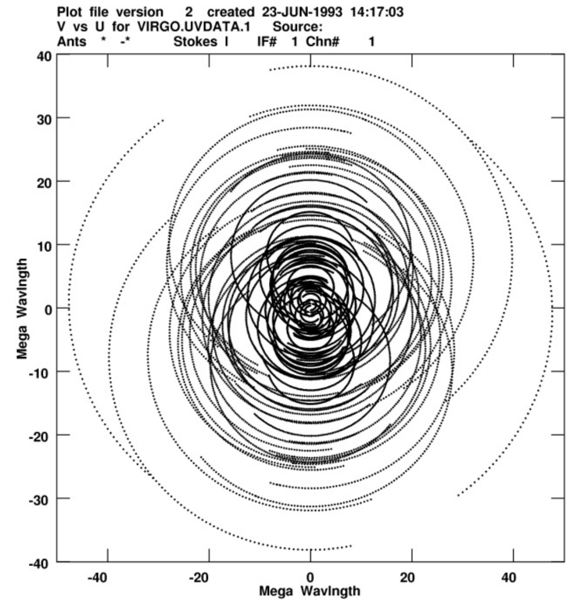

Credit: Tim Cornwell

Aperture synthesis: example

Source model

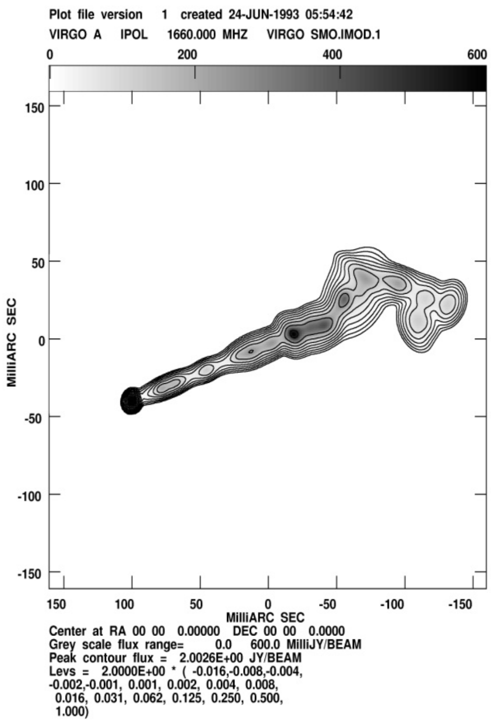

u-v plane

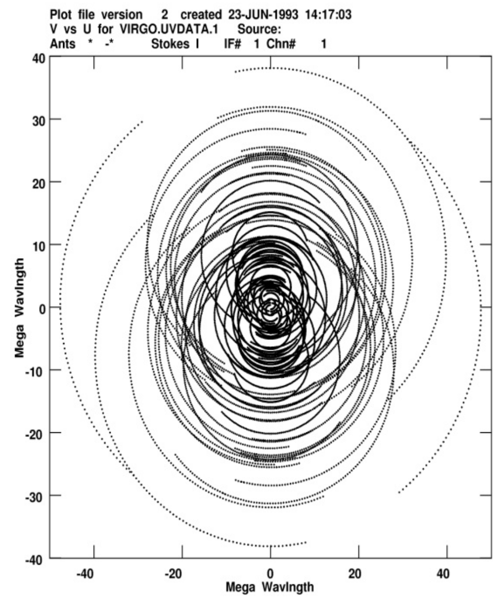

Amplitudes

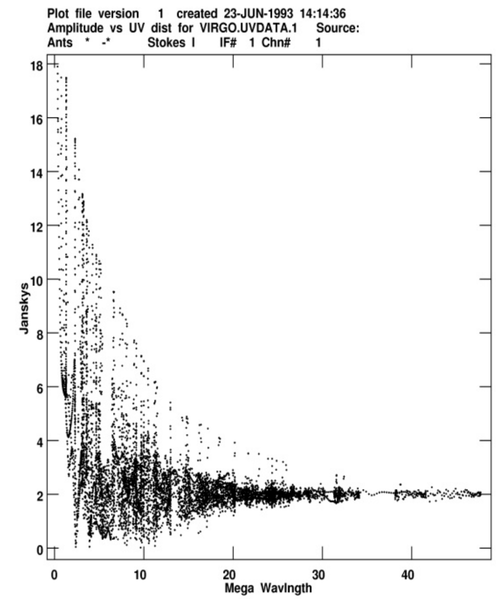

Credit: Tim Cornwell

Aperture synthesis: example

u-v plane

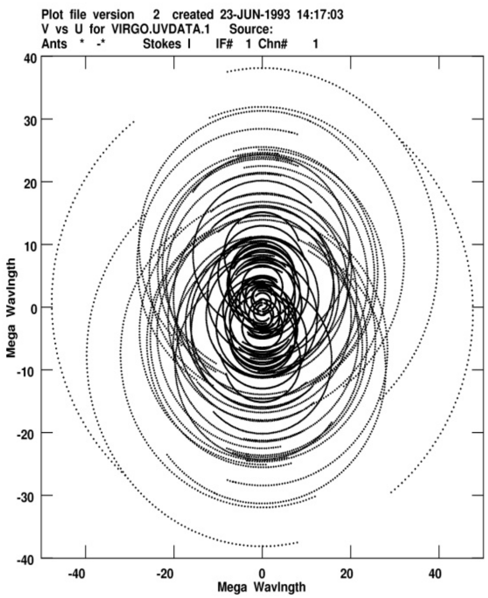

Dirty beam

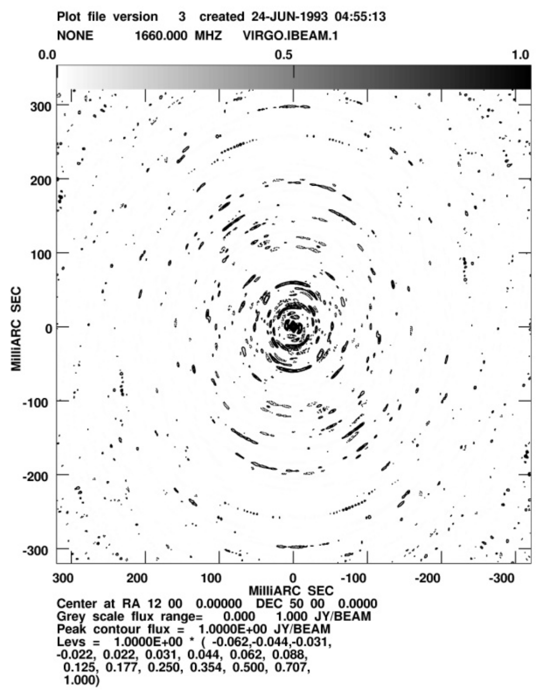

Dirty beam (2-D)

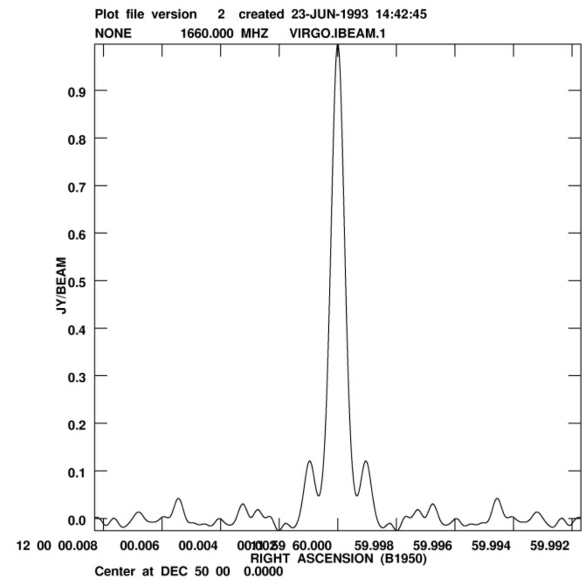

Credit: Tim Cornwell

Aperture synthesis: example

Source model

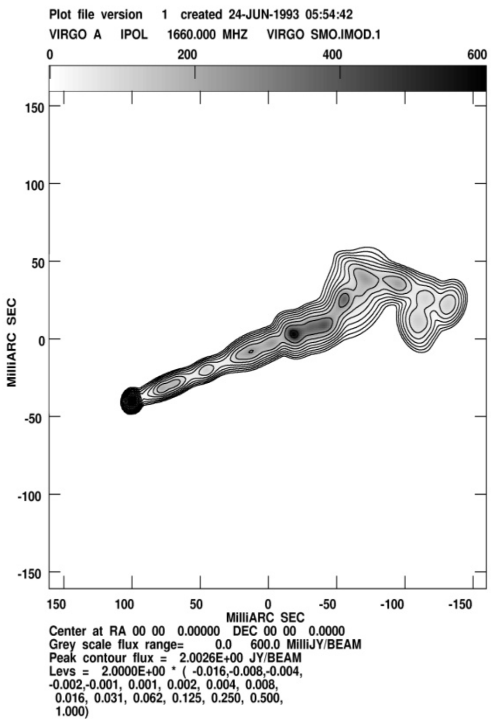

Dirty map

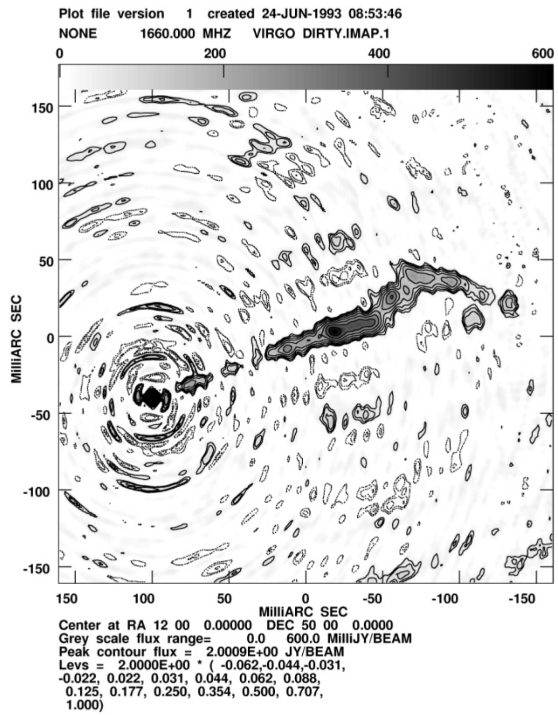

CLEAN map

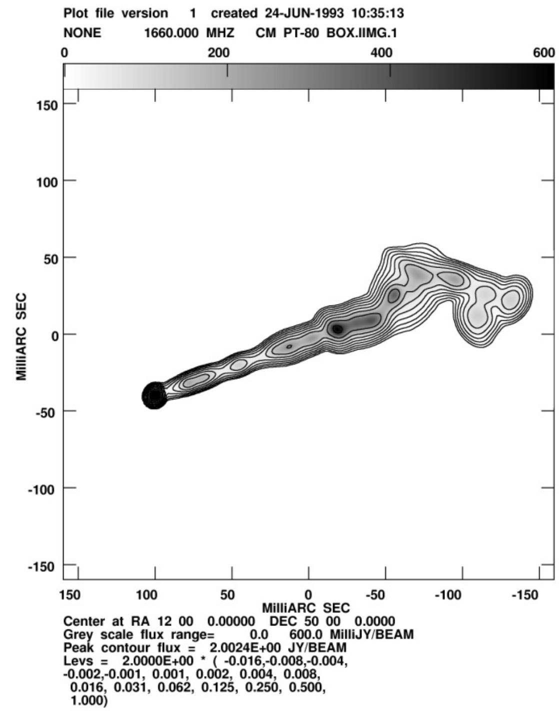

Credit: Tim Cornwell

Another case

Model

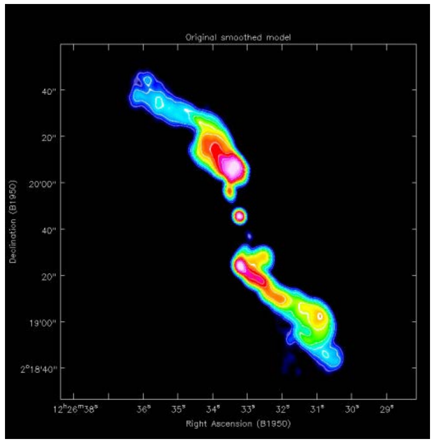

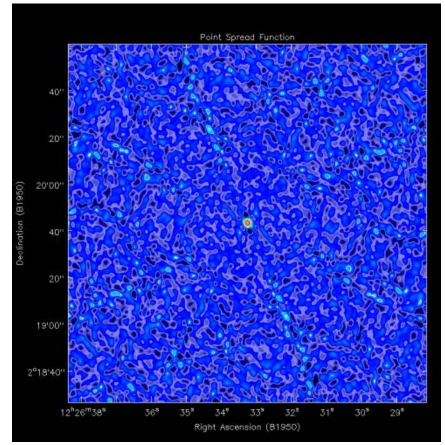

“Dirty” beam

“Dirty” image

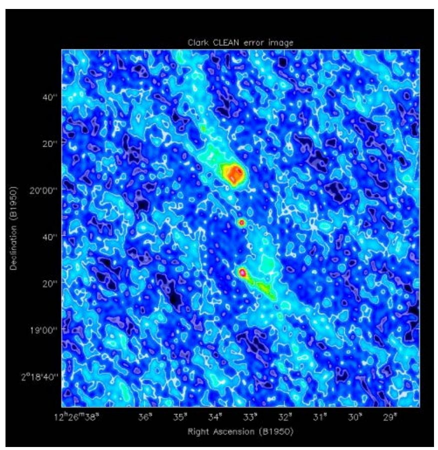

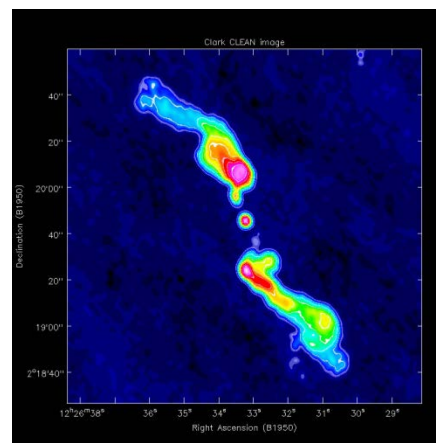

CLEAN image

Credit: Tim Cornwell

VLBI imaging

- Φ cannot be used directly
- Assumes $\Phi_s = 0$ to start (point source)
- Takes advantage of closure phases:
  $\Phi_{1\text{-}2} + \Phi_{2\text{-}3} + \Phi_{3\text{-}1} = f(I(x,y))$
- Iterates to adjust Φ_s

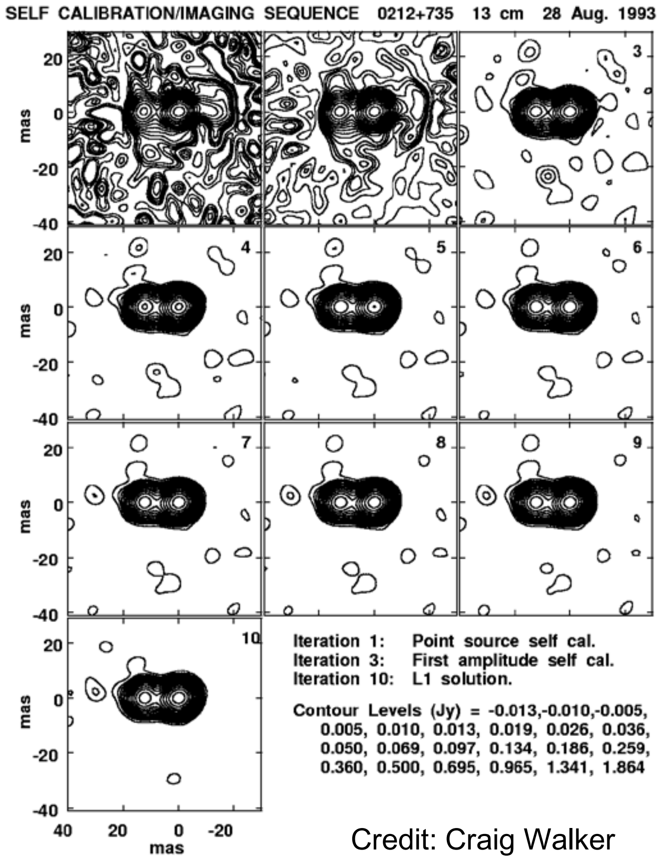

Credit: Craig Walker

VLBI imaging surveys

- Bordeaux VLBI Image Database (2 & 8 GHz)
  http://www.obs.u-bordeaux1.fr/BVID/
- Radio Reference Frame Image Database (2 & 8 GHz)
  http://www.usno.navy.mil/USNO/astrometry/vlbi-products/rrfid
- VLBA Calibrator Survey (2 & 8 GHz)
  http://www.vlba.nrao.edu/astro/calib/index.shtml
- MOJAVE data base (15 GHz)
  http://www.physics.purdue.edu/~mlister/MOJAVE/
- VLBI Imaging and Polarimetry Survey (5 & 15 GHz)
  http://www.phys.unm.edu/~gbtaylor/VIPS/vipscat/vipsncapindx.shtml

Acknowledgements

Information and figures presented in this lecture have been taken from the following sources:

- Mike Garrett's radioastronomy course
  https://www.astron.nl/~mag/dokuwiki/doku.php?id=radio_astronomy_course_description
- NRAO Synthesis Imaging Workshops (2002-2012)
  http://www.aoc.nrao.edu/events/synthesis/2012
- NRAO image gallery
  http://images/nrao.edu/
- Bordeaux VLBI Image Database (2 & 8 GHz)
  http://www.obs.u-bordeaux1.fr/BVID/
- Radio Reference Frame Image Database (2 & 8 GHz)
  http://www.usno.navy.mil/USNO/astrometry/vlbi-products/rrfid
- MOJAVE data base (15 GHz)
  http://www.physics.purdue.edu/~mlister/MOJAVE/